Scientific Research Publishing

Journal of Materials Science and Chemical Engineering, 2024, 12, 119-125
https://www.scirp.org/journal/msce
ISSN Online: 2327-6053
ISSN Print: 2327-6045

Mechanical Evaluation of AZ80 Magnesium Alloy in Cast Wrought Form

Peilin Ying, Anita Hu, Wutian Shen, Henry Hu*

Department of Mechanical, Automotive and Materials Engineering, University of Windsor, Windsor, Canada
Email: yingp@uwindsor.ca, hu14l@uwindsor.ca, shen12a@uwindsor.ca, *huh@uwindsor.ca

How to cite this paper: Ying, P.L., Hu, A., Shen, W.T. and Hu, H. (2024) Mechanical Evaluation of AZ80 Magnesium Alloy in Cast Wrought Form. *Journal of Materials Science and Chemical Engineering*, **12**, 119-125.
https://doi.org/10.4236/msce.2024.124010

Received: March 29, 2024
Accepted: April 27, 2024
Published: April 30, 2024

Abstract

Wrought magnesium alloy AZ80 with a thick section of 20 mm was prepared by squeeze casting (SC) and permanent steel mold casting (PSMC). The porosity measurements of the SC and PSMC depicted that SC AZ80 had a pore content of 0.52%, which was 77% lower than 2.21% of PSMC AZ80 counterpart. The YS, UTS, e_f, E and strengthening rate of cast AZ80 were determined by mechanical pulling. The engineering stress versus strain bended lines showed that SC AZ80 had a YS of 84.7 MPa, a UTS of 168.2 MPa, 5.1% in e_f, and 25.1 GPa in modulus. But, the YS, UTS and e_f of the PSMC AZ80 specimen were only 71.6 MPa, 109.0 MPa, 1.9% and 21.9 GPa. The findings of the mechanical pulling evidently depicted that the YS, UTS, e_f and E of SC AZ80 were 18%, 54%, 174% and 15% higher than PSMC counterpart. The computed resilience and toughness suggested that the SC AZ80 exhibited greater resistance to tensile loads during elastic deformation and possessed higher capacity to absorb energy during plastic deformation compared to the PSMC AZ80. At the beginning of permanent change, the strengthening rate of SC AZ80 was 10,341 MPa, which was 9% greater than 9489 MPa of PSMC AZ80. The high mechanical characteristics of SC AZ80 should be primarily attributed to its low porosity level.

Keywords

Squeeze Casting, Wrought Magnesium Alloy AZ80, Porosity, Tensile Properties

1. Introduction

Considering a substitute of gas or diesel-powered vehicles (GDVs), battery-powered electric vehicles (BEVs) have been increasingly popular on the automotive market owing to exhaust gas emissions causing environmental concerns [1] [2] [3]. However, BEVs are generally heavier than the GDVs. As mass production of

BEVs gains momentum, the imperative to reduce vehicle weight becomes critical, not only for GDVs but also for BEVs aiming for increased mileage with less energy consumption. Consequently, the automotive sector is compelled to explore advanced lightweight materials like magnesium (Mg) alloys. These materials offer a desirable blend of strength and ductility, driving the need for advancements in their manufacturing processes [4] [5] [6].

As the main manufacturing process for Mg alloys, traditional high pressure die-casting processes (C-HPDC) [7] [8] [9] [10] [11] struggled to manufacture components with thick sections due to issues such as entrapped gas and shrinkage pores, oxides, hot tearing, and cold shuts. Consequently, their strength and ductility are reduced.

AZ80 as a wrought Mg alloy can offer an excellent combination of strengths, plasticity, and light weight. But, wrought Mg alloys are typically not castable. Casting wrought alloys presents a significant challenge due to their propensity to develop casting defects like porosity, shrinkage, and hot tearing. These issues arise from their inherent solidification characteristics, characterized by high liquidus temperatures, limited fluidity, susceptibility to hot tearing, and prolonged freezing ranges [11]. Studies on casting of wrought Mg alloy AZ80 with section thickness around 5 mm were attempted and focused on numerical simulation and solidification behavior of rapid cooling. The report on mechanical properties of cast wrought AZ80 alloy with thick section (over 10 mm) is very limited, since the casting defects could easily form in the thick section of cast components. Successful squeeze casting of wrought Al alloys 5083 and 7075 with different section thicknesses and applied pressures has been showcased [12] [13]. This achievement stemmed from the non-critical nature of fluidity and hot tearing as process parameters in squeeze casting. Molten wrought Al alloys solidified within the die cavity under substantial applied pressures, effectively minimizing defects linked to shrinkage and gas pores. However, work on SC of conventional wrought Mg alloys to produce high integrity structural automotive applications with both high strength and excellent plasticity is scarce.

2. Experimental Procedure

2.1. Casting and Material

The selected material was commercially-available magnesium wrought alloy AZ80 containing 8.5 wt% Al, 0.5 wt% Zn and 0.3 wt% Mn. In the process of melt preparation, 450 grams of AZ80 were placed into a steel crucible. This setup operated in the safeguard of protective environment comprising 0.5% SF6 and a balance of CO_2, with a flow rate of 3 standard liters per minute. The AZ80 material was heated to its molten state at 720˚C and maintained at this temperature for 20 minutes. Subsequently, it was stirred for 10 minutes to ensure uniform composition, and any impurities were removed by skimming the surface.

For squeeze casting (SC), the apparatus used was made from an upper and a lower die that are both preheated. The lower die is movable and has a piston to

move molten into the upper die while the upper die is stationary. Molten AZ80, heated to 700˚C, was poured into the lower die, which had been preheated to 300˚C. Once the lower die was raised onto the upper die, heated to 200˚C, the punch piston within the lower die initiated the movement of the melt into the upper die slowly. A 90 MPa pressure was placed on the metal upon the completion of solidification. The SC coupon dimensions were 20 mm in thickness and 100 mm in diameter.

In permanent steel mold casting (PSMC), the process is much simpler. The liquid alloy, with the same weight and sourced from identical heating conditions, was poured into a steel mold to fabricate a rectangular casting plate measuring 150 mm × 125 mm × 20 mm. The steel mold was preheated to 200˚C as well. The PSMC process used gravity to cast AZ80 and protective gas was also used.

2.2. Porosity Measurement

Porosity levels in the alloy were calculated using dry weight (W_d), wet weight (W_w), theoretical (D_t) and actual density (D_a). During porosity measurements, SC and PSMC specimens section from cast coupons sample were sanded and washed to prevent water entrapment on specimen surface. The cleaned specimens were weighted in the air and water to determine W_d and W_w. D_a (ASTM Standard D3800).

$$D_a = \frac{D_w w_a}{W_a - W_w} \tag{1}$$

The pore content of specimens was determined using Equation (2), which involves the measured densities D_t and D_a. Additionally, the porosity of each specimen was calculated based on both theoretical and actual density values, following the procedure outlined in ASTM C948.

$$\%\ \text{Porosity} = \left[\frac{D_t - D_a}{D_t}\right] \times 100\% \tag{2}$$

where D_t represents the theoretical density of AZ80, which is 1806 kg/m^3 [11].

2.3. Mechanical Evaluation

The tensile characteristics of SC and PSMC AZ80 alloys were assessed through tensile testing. Tensile specimens were extracted from SC and PSMC coupons, machined to dimensions compliant with ASTM B557 with a gauge length of one inch 0.0025 m, a thickness of 0.004, and a length of 0.010 m. These prepared specimens underwent tensile testing at room temperature. The tensile machine was configured to a very slow strain rate. Mechanical characteristics, such as yield strength (YS), ultimate tensile strength (UTS), elongation to failure (e_f), elastic modulus (E), resilience (U_r), toughness (U_t), and straining hardening rate, were determined based on the average of three tests. The methodology for calculating resilience, toughness, and straining hardening rate can be found in reference 8.

3. Findings and Comments

3.1. Porosity Assessment

The pore contents of SC and PSMC AZ80 alloys determined based on the Archimedes principle are given in **Figure 1**. As can be seen from **Figure 1**, the SC sample exhibited a porosity level as low as 0.52%, while the porosity in the PSMC was relatively high around 2.21%. Compared to the data given in reference 8, the porosity levels in both the SC and PSMC samples were much lower than that (3.57%) in the C-HPDC Mg alloy AZ91. The variance in pore contents among SC, PSMC, and C-HPDC could be attributed to the dominance of laminar melt flow in SC and PSMC processes. In contrast, the turbulent flow prevailed in the C-HPDC process, which entrapped a large amount of air during cavity filling and resulted in the high porosity level. The air entrapment was reduced by the laminar flow in the SC and PSMC castings. The application of a high pressure (90 MPa) in the SC process squeezed last liquid metal into the porous and shrinkage regions of the solidifying AZ80 casting at the end of solidification, which further reduced the porosity level of the SC sample. In comparison to those of the PSMC and C-HPDC Mg alloys, the SC alloy had the decreases of 325% and 587% in porosity, respectively. The significant reduction in the porosity level should affect its tensile characteristics. Moreover, low porosity level implied that the SC AZ80 could be heat treated to further improve its mechanical properties.

3.2. Mechanical Characteristics

Figure 2 compares the engineering stress-strain curves of the as-cast PSMC and SC AZ80 alloys. It is evident from the figure that SC exhibits a higher UTS, a steeper slope in the linear portion of the engineering curve, and a wider range of elastic and plastic deformation. **Table 1** presents the mechanical properties of PSMC and SC AZ80 alloys, including UTS, YS, e_f, and E, derived from **Figure 2**. The UTS values for PSMC AZ80 and SC AZ80 were 109.0 MPa and 168.2 MPa, respectively, representing a notable 54% improvement from PSMC to SC AZ80. Additionally, the yield strength of SC AZ80, at 84.7 MPa, was 18% higher than that of PSMC AZ80, which had a YS of 71.6 MPa. While the elongation of PSMC

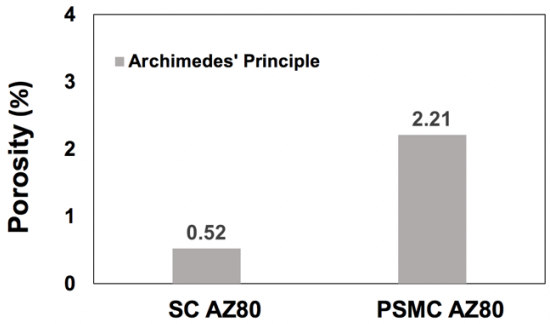

Figure 1. Porosity levels of SC and PSMC AZ80 alloys determined from density measurements and image analyses.

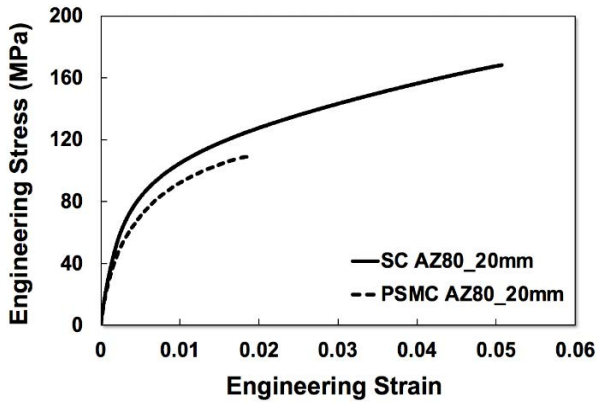

Figure 2. Bended lines of tested alloys describing engineering stress change with strain.

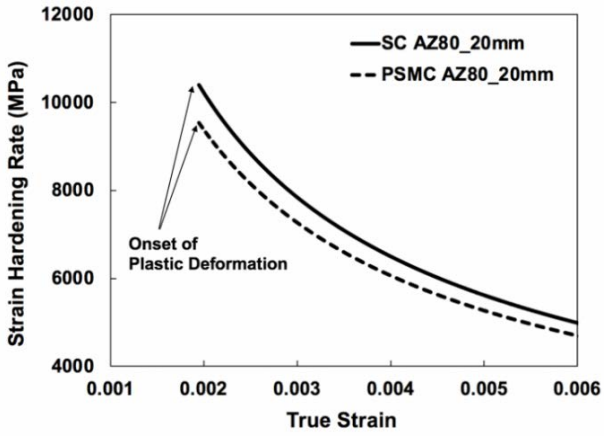

Figure 3. Arcs describing strain-hardening rate change with true strain.

Table 1. Tensile properties of PSMC and SC AZ80.

Casting Method	UTS (MPa)	YS (MPa)	e_f (%)	E (GPa)	U_r (kJ/m^3)	U_t (MJ/m^3)
SC	168.2	84.7	5.1%	25.1	142.8	6.4
PSMC	109.0	71.6	1.9%	21.9	117.2	1.7

alloy was only 1.9%, SC AZ80 exhibited an elongation of 5.1%, marking a substantial 168% increase. The modulus of SC AZ80, at 25.1 GPa, was 15% higher than that of PSMC AZ80, which was 21.9 GPa.

The modulus of resilience and toughness for the PSMC and SC AZ80 alloys are given in **Table 1**. The modulus of resilience for the PSMC AZ80 was 117.2 kJ/m^3 as the SC sample had a toughness of 142.78 kJ/m^3, which was 22% higher. The resilience results indicated that the SC AZ80 was more able to resist tensile loads in engineering application where no permanent distortions were permitted. The PSMC had a toughness value of 1.7 MJ/m^3, while the toughness of the SC specimen was 6.4 MJ/m^3, which was 282% higher than that of the PSMC counterpart. The findings indicated that the SC AZ80 alloy exhibited greater toughness compared to the PSMC AZ80 alloy, as evidenced by its higher UTS, YS, and e_f.

The arcs of strengthening rate concerning plastic strain during tensile pulling plastic for the SC and PSMC samples, extracted from the stress to strain lines are depicted in **Figure 3**. As plastic deformation commenced in Figure, the strengthening rate for SC was 10,341 MPa, while PSMC had a strengthening rate of 9489 MPa. At the beginning of permanent change, the strengthening rate of SC was 9% higher than PSMC. With increasing strain, the strengthening rates of SC and PSMC AZ80 reduced; however, the SC alloy maintained a higher strain-hardening rate compared to its PSMC counterpart. The variation of strengthening rates with true strain implied that SC AZ80 could reinforce itself more rapidly in response to prolonged plastic deformation before fracture compared to the PSMC specimen.

The low pore content of the SC AZ80 given in the preceding section as one of the key factors resulted in its mechanical properties higher than those of the PSMC AZ80. The preliminary microstructure analyses by SEM revealed that, compared to that of the PSMC sample, the microstructure of the SC AZ80 possessed a fine primary dendritic structure, and a large volume fraction of intermetallic phases, which will be published in the near future. The discrepancies in microstructure characteristics between the SC and PSMC alloys likely contribute to the divergent mechanical characteristics and tensile behavior observed, as referenced in literature 3 - 5.

4. Conclusions

- The SC and PSMC processes were employed to cast a wrought magnesium alloy AZ80.
- Due to the high applied pressure and laminar injection of molten alloy, the porosity level (0.5%) of the SC AZ80 alloy was only about one-quarter of that (2.2%) of the PSMC counterpart.
- The SC AZ80 alloy showed the enhanced YS (84.68 MPa), UTS (168.23 MPa), e_f (5.07%), E (25.1 GPa), U_t (6.42 MJ/m^3), and U_r (142.78 kJ/m^3), compared to the PSMC counterpart. The deformation analyses indicated that the hardening phenomenon of the SC AZ80 was evidently strong compared to the PSMC AZ80.
- The porosity level should be partially responsible for the obtained mechanical properties. The superior resistance of the SC alloy to energy loads during elastic deformation was demonstrated. It also exhibited a greater capacity to absorb energy during plastic deformation without fracturing compared to the PSMC AZ80.

Acknowledgements

The research support from the Natural Sciences and Engineering Research Council of Canada and the University of Windsor is fully acknowledged and appreciated.

Conflicts of Interest

The authors declare no conflicts of interest regarding the publication of this paper.

References

[1] Li, Y., Hu, A., Fu, Y., Liu, S., Shen, W., Hu, H. and Nie, X. (2022) Al Alloys and Casting Processes for Induction Motor Applications in Battery-Powered Electric Vehicles: A Review. *Metals*, **12**, 216-241. https://doi.org/10.3390/met12020216

[2] Shen, W., Hu, A., Liu, S. and Hu, H. (2023) Al-Mn Alloys for Electrical Applications: A Review. Journal of Alloys and Metallurgical Systems, **2**, 100008. https://doi.org/10.1016/j.jalmes.2023.100008

[3] Yavas, A., Cilingir, C., Turk, A. and Celik, E. (2023) Production and Characterization of Highly Conductive Aluminum Metal for Electric Motor Applications. *Journal of Materials Engineering and Performance*. https://doi.org/10.1007/s11665-024-09154-7

[4] Wang, G.G., Weiler, J.P. (2023) Recent Developments in High-Pressure Die-Cast Magnesium Alloys for Automotive and Future Applications. *Journal of Magnesium and Alloys*, **11**, 78-87. https://doi.org/10.1016/j.jma.2022.10.001

[5] Liu, B., Yang, J., Zhang, X., Yang, Q., Zhang, J. and Li, X. (2023) Development and Application of Magnesium Alloy Parts for Automotive OEMs: A Review. *Journal of Magnesium and Alloys*, **11**, 15-47. https://doi.org/10.1016/j.jma.2022.12.015

[6] Yang, Y., Xiong, X., Chen, J., Peng, X., Chen, D. and Pan, F. (2021) Research Advances in Magnesium and Magnesium Alloys Worldwide in 2020. *Journal of Magnesium and Alloys*, **9**, 705-747. https://doi.org/10.1016/j.jma.2021.04.001

[7] Zeng, Z., Salehi, M., Kopp, A., Xu, S., Esmaily, M. and Birblis, N. (2022) Recent Progress and Perspectives in Additive Manufacturing of Magnesium Alloys. *Journal of Magnesium and Alloys*, **10**, 1511-1541. https://doi.org/10.1016/j.jma.2022.03.001

[8] Fu, Y., Li, Y., Hu, A., Hu, H. and Nie, X. (2020) Microstructure, Tensile Properties and Fracture Behavior of Squeeze-Cast Mg Alloy AZ91 with Thick Cross Section. *Journal of Materials Engineering and Performance*, **29**, 4130-4141. https://doi.org/10.1007/s11665-020-04910-x

[9] Thakur, B., Barve, S. and Pesode, P. (2023) Investigation on Mechanical Properties of AZ31B Magnesium Alloy Manufactured by Stir Casting Process. *Journal of the Mechanical Behavior of Biomedical Materials*, **138**, 105641. https://doi.org/10.1016/j.jmbbm.2022.105641

[10] Sun, Z., Geng, X., Ren, L. and Hu, H. (2020) Microstructure, Tensile Properties and Fracture Behavior of HPDC Magnesium Alloy AZ91. *International Journal of Materials, Mechanics and Manufacturing*, **8**, 50-56. https://doi.org/10.18178/ijmmm.2020.8.2.483

[11] Avedesian, M.M. and Baker, H. (1999) Magnesium and Magnesium Alloys. ASM International, Metals Park, OH.

[12] Zhang, X., Fang, L., Hu, H., Nie, X. and Tjong, J. (2017) Interfacial Heat Transfer of Squeeze Casting of Wrought Al Alloy 5083 with Variation in Wall Thicknesses. *Advances in Materials and Processing Technologies*, **3**, 407-417. https://doi.org/10.1080/2374068X.2017.1336352

[13] Zhang, X., Fang, L., Hu, H., Nie, X. and Tjong, J. (2017) Determination of Metal/Die Interfacial Heat Transfer Coefficients in Squeeze Casting of Wrought Al Alloy 7075 with Variations in Section Thicknesses and Applied Pressures. *ASME Journal of Heat and Mass Transfer*, **139**, 022101-1-9. https://doi.org/10.1115/1.4034855